

Low-frequency spectroscopy of superconducting photonic crystals

A.N. Poddubny^{a*}, E.L. Ivchenko^a, Yu.E. Lozovik^b

^a *A.F. Ioffe Physico-Technical Institute, 194021 St. Petersburg, Russia*

^b *Institute of Spectroscopy, 142190 Troitsk, Moscow region, Russia*

Transmission, reflection and absorption of electromagnetic radiation and photon dispersion law for 2D photonic crystals with superconducting elements are studied. The calculation of optical properties of photonic crystals is studied by layer-by-layer Korringa-Kohn-Rostoker techniques. The results of numerical calculations performed for an array of superconducting cylinders have been understood in terms of a simple analytical model. The controlling of optical properties of superconducting photonic crystal by temperature and magnetic field is discussed. The variation of superconducting component density with temperature leads, particularly, to significant reduction of the transmission peaks and even to a nonmonotonous behavior of some absorbance peaks.

PACS numbers: 42.70.Qs, 74.25.Gz, 74.78.-w

Keywords: Optical properties, Light reflection and absorption, High- T_c superconductors

I. INTRODUCTION

Photonic crystals (PCs) consisting of metallic wires are a subject of growing interest during last years and are widely studied both theoretically [1,2,3,4,5] and experimentally [6,7]. At low-frequencies, e.g., in the giga- and terahertz spectral regions, the real part of the dielectric function of metallic component is large and negative which allows the formation of the complete two-dimensional photonic band gap in these spectral regions. Moreover, the electromagnetic waves cannot propagate in such a system at frequencies lower than the so-called cutoff frequency ω_c [2]. If lattice constant of these structures lies in the millimeter and submillimeter ranges their fabrication is relatively simple. However, the damping of electromagnetic waves in metals can suppress many potentially useful properties of metallic PCs. The possible solution of this problem is the replacement of the PC metallic component by a superconducting (SC) component. The dielectric function depends on superconducting gap Δ (see, e.g., Refs. [8,9] and references therein) and SC state can be varied by alteration of external parameters, such as temperature and external magnetic field which provide a method for a control of the optical properties of metallic PCs. The dielectric losses are reduced essentially below superconducting transition in SC state, and recent experiments have shown that photonic band edges become sharper in SC metals [7].

The band structure of a superconducting PC was analyzed in Ref. [8]. Here we calculate the transmission, reflection, and absorption spectra and analyze controlling of these spectra by temperature.

II. PROBLEM DEFINITION AND METHOD OF CALCULATION

We study the photonic crystal formed by a periodic array of parallel superconducting cylinders with radius R arranged in a square lattice with the lattice constant a , see Fig. 1. Electromagnetic waves propagating in this structure are described by Maxwell equation

$$\nabla \times \nabla \times \mathbf{E}(\mathbf{r}) = \left(\frac{\omega}{c}\right)^2 \varepsilon(\mathbf{r}, \omega) \mathbf{E}(\mathbf{r}) \quad (1)$$

where $\varepsilon(\mathbf{r}, \omega)$ is the dielectric function equal to that of the superconducting metal inside the cylinders and to unity outside them (in vacuum). For simplicity, we consider the electro-magnetic response of superconductor cylinders by using the two-liquid Gorter-Kazimir model and describe the electronic system as an admixture of two independent carrier liquids, superconducting and normal. With the increasing of temperature T or magnetic field \mathbf{B} , the density of the normal component, n_n , increases at the expense of the superfluid component, n_s , because the total density of electrons $n_{tot} = n_n + n_s$ is conserved.

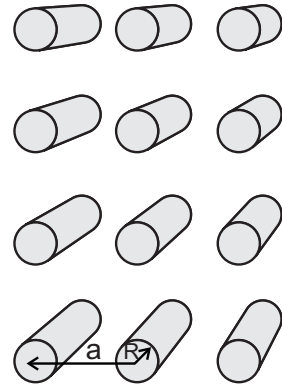


FIG. 1: Schematic representation of a two-dimensional photonic crystal with cylinders of the radius R arranged in a square lattice with the lattice constant a .

*E-mail address: poddubny@coherent.ioffe.ru

At the critical temperature $T = T_c$ only normal phase survives whereas, at zero temperature, only superfluid phase does exist.

In the Gorter-Kazimir model the dielectric function of a superconductor can be presented in the following simple form

$$\varepsilon_{\text{GK}}(\omega) = 1 - \omega_p^2 \left(\frac{\alpha}{\omega^2} + \frac{1 - \alpha}{\omega(\omega + i\gamma)} \right) \quad (2)$$

where ω_p is the plasma frequency $(4\pi n_{\text{tot}} e^2 / m)^{1/2}$ corresponding to the total electron density n_{tot} , m is the electron effective mass, γ is the phenomenological damping coefficient describing the relaxation of normal electron component, and α is the fraction of superconducting component n_s / n_{tot} which varies continuously with temperature (at magnetic field $H = 0$) from $\alpha = 1$ at $t = 0$ to $\alpha = 0$ at $T = T_c$. It can be controlled also by magnetic field. It should be noted, that this equation is valid qualitatively for the frequencies ω below the superconducting gap 2Δ .

At the critical temperature T_c or critical magnetic field H_{cr} the superconducting phase vanishes and the dielectric function can be described by the conventional Drude equation

$$\varepsilon_{\text{GK}}(\omega) = 1 - \frac{\omega_p^2}{\omega(\omega + i\gamma)}$$

In the opposite limit, $T \rightarrow 0$, the contribution of the normal component is negligible and the dielectric function reduces to

$$\varepsilon_{\text{GK}}(\omega) = 1 - \frac{\omega_p^2}{\omega^2}$$

In numerical calculations we consider high-temperature superconductor YBaCuO; its parameters in the normal state are as follows: $\omega_p = 1.67 \times 10^{15}$ rad/s, $\gamma = 1.34 \times 10^{13}$ rad/s. For YBaCuO the superconducting gap can be estimated as $2\Delta \approx 6k_B T_c / \hbar$ (k_B is the Boltzmann constant). For $T_c = 91$ K one has $\Delta = 28$ meV which is equivalent to 7 THz. A value of 150 μm is chosen for the lattice constant a so that frequencies of the first few allowed photonic bands lie below Δ . The filling factor $f = \pi(R/a)^2$ in our calculations is equal to 5%.

The optical spectra are calculated for finite-size two-dimensional PC slab with the normal parallel to the symmetry direction $\langle 01 \rangle$. In this case the structure can be considered as N identical layers, each containing one-dimensional chain of cylinders. In what follows we restrict ourselves to the case of normal incidence of TE-polarized light, which means that the electric field is parallel to the cylinder axis z , $\mathbf{E} = (0, 0, E_z)$. In this particular geometry Eq. (1) can be rewritten as

$$\left[\frac{\partial^2}{\partial x^2} + \frac{\partial^2}{\partial y^2} + \left(\frac{\omega}{c} \right)^2 \varepsilon(x, y; \omega) \right] E_z(x, y) = 0 \quad (3)$$

The numerical calculation is performed by a two-dimensional bulk and layer-by-layer Korringa-Kohn-Rostoker techniques [10].

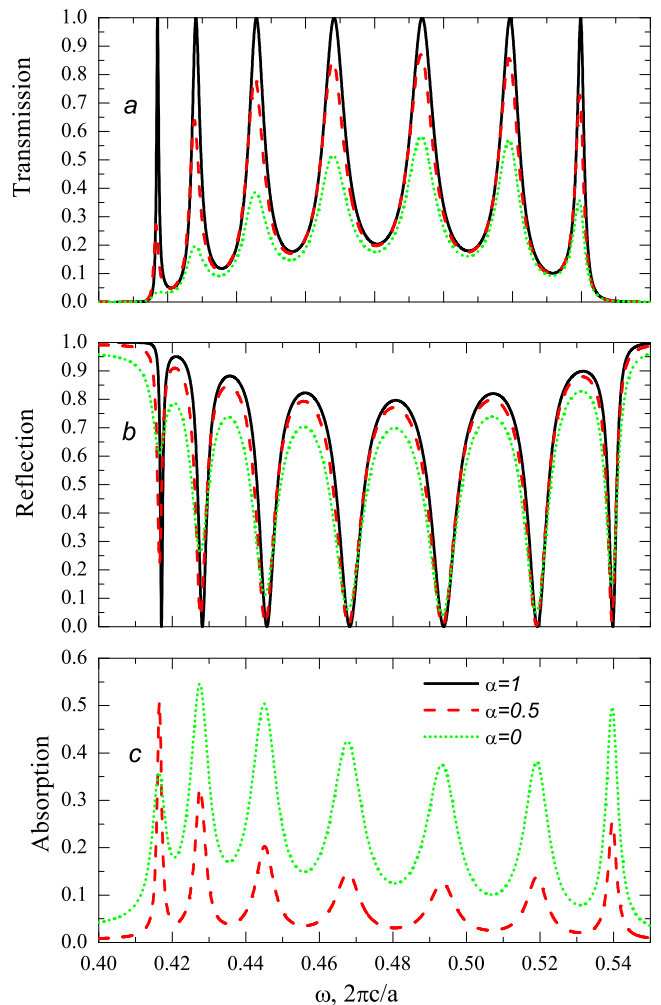


FIG. 2: Transmission (a), reflection (b), and absorption (c) spectra of a superconducting photonic crystal calculated for three different values of α and the set of other parameters given in the text. At $\alpha = 1$ the absorption is zero and the corresponding line $A(\omega) \equiv 0$ coincides with the abscissa.

III. RESULTS AND DISCUSSION

Figure 2 presents the transmission, reflection and absorption spectra, respectively, $T(\omega)$, $R(\omega)$ and $A(\omega) = 1 - R(\omega) - T(\omega)$, for a 8-layer-thick superconducting PC calculated for different values of parameter α . The chosen spectral region covers the first allowed band, diffraction channels at these frequencies are closed. For the pure SC phase, $\alpha = 1$, the absorption vanishes, $R(\omega) = 1 - T(\omega)$, and the transmission peak values reach unity. With decreasing α the transmission and reflection at any fixed ω decrease monotonously, with the transmission being more sensitive to the variation of α . At the same time the absorption maximum can exhibit a non-monotonous behavior, at least it is the case for the first absorption peak. For the chosen lattice constant the parameter $2\pi c/a$ is comparable with the attenuation γ , the role of the elec-

tronic relaxation is significant except for very low fraction of normal electrons, i.e. except for the region $1 - \alpha \ll 1$. The oscillations in optical spectra can be interpreted in terms of the interference effects taking into account the modification of the photonic dispersion in the PCs. Such spectral behavior is typical for metallic PCs, see, e.g., [4]. However, for the THz frequency region considered here, the values of $|\varepsilon_{\text{GK}}(\omega)|$ are of the order of 10^4 which is by almost three orders of magnitude larger than for the optical region studied in [4].

Below we propose a simple analytical description of photonic modes near the edge of the allowed photonic band where the photon frequency and two-dimensional Bloch wave vector $\mathbf{k} = (k_x, k_y)$ are related by

$$\omega = \omega_0 + Ck^2. \quad (4)$$

Here the zero- k frequency ω_0 and the coefficient Ω have imaginary contributions if $\text{Im}\{\varepsilon_{\text{GK}}(\omega)\} \neq 0$. Taking into account that at low frequencies real part of $\varepsilon_{\text{GK}}(\omega)$ is negative and its modulus is very large, we can expand ω_0 and C in powers of $1/\sqrt{-\varepsilon_{\text{GK}}}$. In the first-order approximation we obtain instead of Eq. (4)

$$\omega = \omega_0^\infty - \frac{\Omega}{\sqrt{-\varepsilon_{\text{GK}}(\omega_0^\infty)}} + \left(\eta + \frac{\zeta}{\sqrt{-\varepsilon_{\text{GK}}(\omega_0^\infty)}} \right) (ck)^2, \quad (5)$$

where c is the light velocity in vacuum (introduced here for convenience), ω_0^∞ and $c^2\eta$ are the values of ω_0 and C in the limit $\varepsilon_{\text{GK}} \rightarrow \infty$. It should be stressed that the parameters ω_0^∞ , Ω , η and ζ depend only on the geometry of the system and are independent of the cylinder dielectric function ε_{SC} . More precisely, one can use the representation

$$\omega_0^\infty = s_1 \frac{2\pi c}{a}, \quad \Omega = s_2 \frac{2\pi c}{a}, \quad \eta = s_3 \frac{a}{2\pi c}, \quad \zeta = s_4 \frac{a}{2\pi c},$$

where the coefficients s_1 to s_4 depend only on the ratio R/a . The fitting of the first-allowed-band dispersion curves obtained for different values of ε_{SC} give the following values

$$s_1 = 0.415, \quad s_2 = 0.63, \quad s_3 = 0.98, \quad s_4 = 3.45.$$

Equation (5) can be compared to the corresponding expansion for a planar waveguide near the cutoff frequency, see [11]. For an ideal planar waveguide of the thickness d , one has

$$\omega = c\sqrt{\left(\frac{\pi}{d}\right)^2 + k^2} \approx \frac{\pi c}{d} + \frac{d}{2\pi c} (ck)^2.$$

The cutoff frequency and coefficient η are equal to $\pi c/d$ and $d/2\pi c$, respectively. On the other hand, for the PC under study, the frequency ω_0^∞ is close to $\pi c/a$ (or, equivalently, $s_1 \approx 0.5$) and $s_3 \approx 1$. This helps the interpretation of Eq. (5), namely, in the PC the effective waveguide ‘‘boundaries’’ are the planes containing cylinders. When

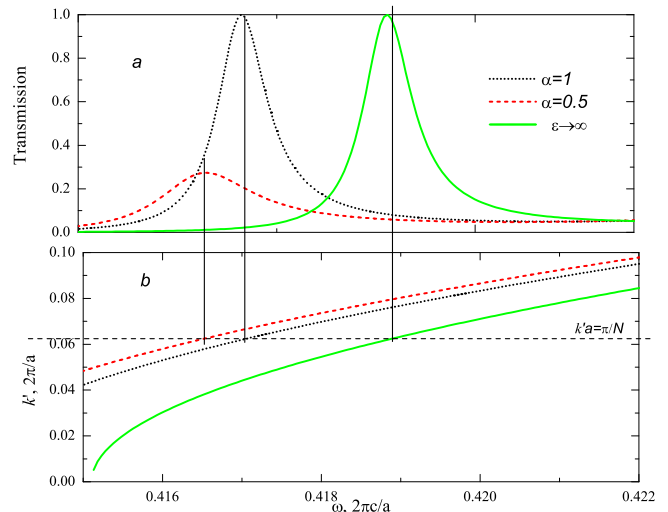


FIG. 3: (a) Transmission spectrum $T(\omega)$ and (b) photon dispersion $k'(\omega)$ near the first transmission peak. Solid, dashed and dotted curves are calculated for $\alpha = 1$, $\alpha = 0.5$, and $|\varepsilon_{\text{SC}}| \rightarrow \infty$. Other parameters including $N = 8$ are the same as in Fig. 2. The vertical lines indicate the frequencies at which $k'(\omega) = \pi/(Na)$, this value of k' is indicated by a horizontal line.

the waveguide is not ideal, i.e., the dielectric constant is negative, large but finite, the radiation slightly penetrates in its walls which leads to an increase in the effective thickness d and a decrease in the cutoff frequency, in agreement with the positive sign of Ω .

The relation between the transmission peak position and the photon dispersion is analyzed in Fig. 3. Figure 3a presents the first transmission peak for the PC structures with $\alpha = 0.5$, $\alpha = 1$ and $\varepsilon_{\text{SC}} \rightarrow \infty$. The first two lines are fragments of those shown in Fig. 2a. The third line corresponding to $\varepsilon_{\text{SC}} \rightarrow \infty$ (equivalent to the boundary condition $E_z(\boldsymbol{\rho}) = 0$ at the cylinder surfaces) looks like a slightly blue-shifted spectrum of the purely SC PC. A value of the shift is in agreement with the estimation $\Omega [-\varepsilon_{\text{GK}}(\omega_0^\infty; \gamma = 0)]^{-1/2}$ that follows from Eq. (5). This equation also allows one to understand the evolution of the spectrum with decreasing α : for α different from unity the photon wave vector acquires an imaginary part and the transmission decreases. The similar analysis clearly shows that the spectral position of the transmission maxima in Fig. 2 are determined by the Fabry-Pérot interference condition

$$Nk'(\omega_m)a = m\pi, \quad m = 1, 2 \dots N - 1, \quad (6)$$

where $k'(\omega_m)$ is the real part of the photon wave vector at the frequency ω_m . Thus, the peaks in the transmission spectrum can be related to the Fabry-Pérot interference. Extending this one-dimensional interpretation we can apply the approximate estimation for the transmission and

reflection coefficients

$$T_N(\omega) = \frac{e^{-2k''(\omega)aN}|1-r^2|^2}{|1-r^2e^{2ik(\omega)aN}|^2}, \quad (7)$$

$$R_N(\omega) = \frac{|r(1-e^{2ik(\omega)aN})|^2}{|1-r^2e^{2ik(\omega)aN}|^2}$$

derived for a slab of the thickness Na . Here k'' is the imaginary part of the wave vector $k(\omega)$ calculated for the photonic crystal and r is the internal reflection coefficient considered as a fitting parameter while making a comparison with the exact calculation. Equation (6) implies the condition $r'' = 0$ and, for lowest peak with $m = 1$, the fit gives $r \approx 0.84$.

The two-dimensional nature of the PC makes it difficult to derive a stricter analytical equations for the spectra, but the key features of their dependence on α , in particular, the red shift and decrease of the absolute value of the transmission are quite well reproduced by Eqs. (7) with $k(\omega)$ determined from Eq. (5). Fig. 4 presents the same curves as Fig. 2 but in large scale and only in the vicinity of the peak $m = 1$. One can see that dashed curves, calculated by the approximate equations (7) lie sufficiently close to the exact ones. Expressions (7) can be simplified in the spectral region near each frequency ω_m satisfying Eq. (6). Assuming $1 - r \ll 1$ and $k''aN \ll 1$, we can reduce Eqs. (7)

$$T_N(\omega) \approx \frac{\Gamma_m^{(0)2}}{(\omega - \omega_m)^2 + (\Gamma_m^{(0)} + \Gamma_m)^2}, \quad (8)$$

$$R_N(\omega) \approx \frac{\Gamma_m^2 + (\omega - \omega_m)^2}{(\omega - \omega_m)^2 + (\Gamma_m^{(0)} + \Gamma_m)^2},$$

$$A_N(\omega) \approx \frac{2\Gamma_m\Gamma_m^{(0)}}{(\omega - \omega_m)^2 + (\Gamma_m^{(0)} + \Gamma_m)^2},$$

with

$$\Gamma_m = k''(\omega_m)aN\Delta, \quad \Gamma_m^{(0)} = (1-r)\Delta, \quad (9)$$

$$\Delta = \frac{1}{aN} \left[\frac{dk'(\omega_m)}{d\omega} \right]^{-1}.$$

It follows then that narrow peaks in the transmission and absorption as well as narrow dips in the reflection can be described in terms of resonant tunneling in the region of a “confined”-photon eigenfrequency ω_m . Consequently, $\Gamma_m^{(0)}$ and Γ_m mean the radiative and non-radiative decay rates of the corresponding “confined” state m . The non-radiative decay vanishes for $\alpha = 1$ and increases with decreasing α which leads to a broadening of the peaks. The peaks near the middle of the allowed band are wider than those near the edge, as clearly seen in Fig. 2c, which is due to the larger values of $\Delta \propto d\omega/dk'$. Note that, although the integral over the absorption spectrum (8) monotonously increases with $\Gamma_m(\alpha)$, the peak value of $A_N(\omega)$ has a maximum at $\Gamma_m(\alpha) = \Gamma_m^{(0)}$, i.e., $A_N(\omega_m, \Gamma_m = \Gamma_m^{(0)}) = 1/2$. Analogous behavior of the

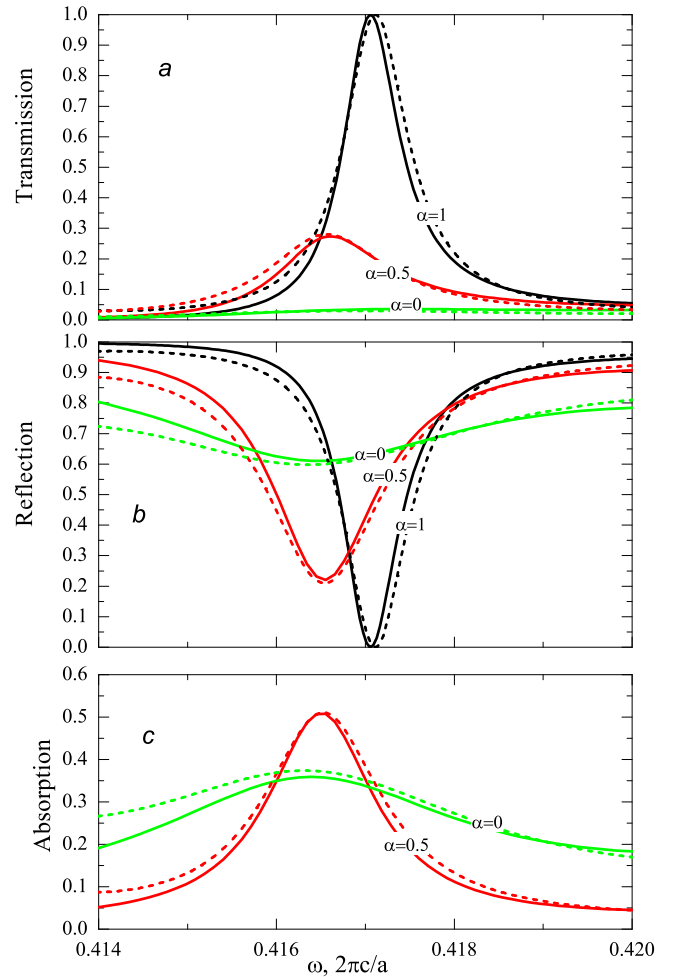


FIG. 4: Transmission (a), reflection (b), and absorption (c) spectra of a superconducting photonic crystal calculated for three indicated values of α and the same set of parameters as in Fig. 2. Solid and dashed curves correspond to spectra calculated numerically and by using Eqs. (7). At $\alpha = 1$ the absorption is zero, the corresponding line $A(\omega) \equiv 0$ coincides with the abscissa and is indistinguishable.

absorption peaks was observed for the two-dimensional photonic crystal consisting of spherical voids buried in a metal film [12]. If we take into account overlapping between peaks (8) with different m the maximum value of the absorbance can slightly exceed $1/2$, as is seen in Fig. 2c.

IV. CONCLUSION

We have studied the photon dispersion law and optical properties of a two-dimensional superconducting photonic crystal formed by metallic cylinders arranged in a square lattice. The transmission, reflection and absorption spectra are calculated as a function of the fraction α of superconducting electrons. In the spectral region within the allowed band the spectra exhibit oscillations

due to the interference effects. For the pure SC phase, $\alpha = 1$, the absorption vanishes, $R(\omega) = 1 - T(\omega)$, and the transmission peak values reach unity. With the transition from superconducting to normal metallic phase when α changes from 1 to 0 the optical spectra exhibit remarkable modifications. The proposed approximate analytical description allows one to explain the key features of the dispersion and spectral modifications with changing α . The peaks in transmission and absorption spectra as well

as the dips in the reflection spectra can be interpreted in terms of the resonance tunneling.

Acknowledgments

The work was supported by RFBR and the “Dynasty” foundation – ICFPM.

-
- ¹ A.L. Pokrovsky, A.L. Efros, Phys. Rev. Lett. 89 (2002) 93901.
- ² J.B. Pendry, A.J. Holden, W.J. Stewart, I. Youngs, Phys. Rev. Lett. 76 (1996) 4773.
- ³ K. Sakoda, N. Kawai, T. Ito, A. Chutinan, S. Noda, T. Mitsuyu, K. Hirao, Phys. Rev. B 64 (2001) 45116.
- ⁴ Zhenlin Wang, C.T. Chan, Weiyi Zhang, Naiben Ming, Ping Sheng, Phys. Rev. B 64 (2001) 113108.
- ⁵ A. A. Krokhin, E. Reyes, and L. Gumen, Phys. Rev. B. 75 (2007) 045131.
- ⁶ A. Pimenov, A. Loidl, Phys. Rev. Lett. 96 (2006) 63903.
- ⁷ M. Ricci, N.Orloff, S. M. Anlage, Appl. Phys. Lett. 87 (2005) 34102.
- ⁸ O.L. Berman, Yu.E. Lozovik, S.L. Eiderman, R.D. Coalson, Phys. Rev. B 74 (2006) 92505.
- ⁹ A.L.Dobryakov, V.M.Farztdinov, Yu.E.Loizovik, Phys.Scr., 60, (1999) 474.
- ¹⁰ K. Ohtaka, T. Ueta, K. Amemiya, Phys. Rev. B 57 (1997) 2550.
- ¹¹ M.M. Sigalas, C.T. Chan, K.M. Kho, C.M. Soukulis, Phys. Rev. B 52 (1996) 11744.
- ¹² T.V. Teperik, V.V. Popov, F.J. García de Abajo, phys. stat. sol. (a) 202 (2005) 362.